Optical and Quantum Electronics (2023) 55:692
https://doi.org/10.1007/s11082-023-04988-2

Deep learning based BER improvement for NOMA-VLC systems with perfect and imperfect successive interference cancellation

Wessam M. Salama[1] · **Moustafa H. Aly**[2] · **Eman S. Amer**[3]

Received: 23 March 2023 / Accepted: 20 May 2023 / Published online: 8 June 2023

Abstract

This paper focuses in the improvement of the BER performance of multiple-input multiple-output (MIMO) systems is investigated utilizing non-orthogonal multiple access-visible light communication (NOMA-VLC). Applying multi-user downlink MIMO-NOMA-VLC system within equal gain combiner at the receiver is used with two types of modulation; On–Off Keying (OOK) and L-Pulse Position Modulation, with L = 4 and 8. The perfect and imperfect successive interference cancellation scenario is used in this system, and the scenario is considered for two and three users. Our proposed framework is divided into two stages. First, data is collected using the MATLAB software. Second, two deep learning models (DLMs); ResNet50V2 and InceptionResNetV2 which are trained and tested. Python software is then used to develop and train the DLMs. The obtained results assures the superiority of ResNet50V2 over InceptionResNetV2, in different cases and for all users. The BER performance is also studied versus α for two and three users OOK modulation single-input single-output (SISO), (2 × 2) and (3 × 2) MIMO-NOMA-VLC systems based on the two DL techniques; ResNet50V2 and InceptionResNetV2. Again, ResNet50V2 achieves better results than InceptionResNetV2. The obtained results are compared with the previously published ones, showing that the proposed system and techniques achieve better results.

Keywords Non-orthogonal multiple access (NOMA) · Single-input single-output (SISO) · Multiple-input multiple-output (MIMO) · Deep learning models (DLMs) · Visible light communication (VLC) · Successive interference cancellation (SIC)

✉ Moustafa H. Aly
mosaly@aast.edu

[1] Department of Computer Engineering, Faculty of Engineering, Pharos University, Alexandria, Egypt

[2] Arab Academy for Science, Technology and Marine Transport, Alexandria, Egypt

[3] High Institute for Engineering and Technology, King Mariout, Alexandria, Egypt

1 Introduction

Visible Light Communication (VLC) provides a wide range of spectrum, easy accessibility, high data rate, high power efficiency and other advantages that qualifies VLC to achieve the revolution in the next years. Several techniques in wireless communication have used VLC systems for its huge data rate and low bit error rate (BER).

Several researchers are interested in the field of NOMA-MIMO-VLC, where Dixit et al. demonstrated the analysis of BER for an angular diversity receiver utilizing MIMO-VLC (Dixit and Kumar 2021a, b). In Al-Nahhal et al. (2019), authors aimed to increase the spectral efficiency within MIMO-VLC using Orthogonal Frequency Division Multiplexing (OFDM). MIMO-OFDM-VLC was used in implementation of the wrap phase technique in Al-Nahhal et al. (2021). MIMO-OFDM-VLC system was used for optimization the spectral efficiency in Siddiqi et al. (2020). NOMA is a recent technique that used for providing extra spectral efficiency depending on Superposition Coding (SC) for multiplexing the transmitted signals in power domain. While at receiver, SIC with multiple users was applied to decode the received signal. The BER performance for NOMA-OFDM-VLC systems was analyzed in Lin (2017). Different modulation techniques were used for studying BER for NOMA-VLC as M-QAM, square QAM, M-PAM, and M-PSK in LiU et al. (2019), Almohimmah and Alresheedi (2020).

The SIC was also investigated to improve the performance of NOMA-VLC systems in Dixit and Kumar (2021a, b). To enhance the performance of NOMA-VLC, the MIMO technique was used to decrease the BER. In Chen et al. (2018), a NOMA-MIMO-VLC was presented using the power allocation method which improved the data rate. Also, in Mitra and Bhatia (2017), a recent precoder design was used to improve the performance of the NOMA-MIMO-VLC system. Recently, Artificial Intelligence (AI) has been used for improving the performance of several fields.

To study NOMA optical wireless communication systems, two major Machine Learning (ML) branches are now widely used. As shown in Bhatt et al. (2022), Deep Learning (DL) can be used to deal with the complexity of mathematical modeling and overcome nonlinear distortion in NOMA optical wireless communication systems for signals. By extracting features from large amounts of training data and optimizing system performance, DL, as a sub-branch of ML, can provide a data-driven solution to this problem (Tian et al. 2022). The DL network can replace the mathematical model in such a system. Although it is unclear whether DL-based wireless communication outperforms traditional wireless communication in terms of performance improvement and complexity, DL-based algorithms are thought to be faster and consume less power than the traditional ones.

Many fields have successfully applied DL technology, which can automatically learn more complex features from complex data structures, including signal classification, modulation recognition (O'Shea et al. 2016), sentiment analysis (Song et al. 2018), channel estimation (Soltani et al. 2019), and image processing (Ngo et al. 2021). Recently, a significant progress has been achieved in the quantization and feedback of MIMO channels, and certain channel state (CS) technology issues have been resolved; thanks to the DL approach (Qi and Su 2022; An et al. 2022; Kaur et al. 2022). The NOMA spectrum used in radio frequency (RF) for free space optical networks has been improved in Zaki et al. (2022), Upadhya et al. (2022). In terms of underwater networks, most NOMA research focuses on improving the receiving rates and performance, with channel studies occurring infrequently (Ai et al. 2022). DL was used to solve the NOMA scheme of an indoor VLC system (Ullah et al. 2022).

Our target in this article is to adopt AI to improve the NOMA-MIMO-VLC system performance.

The main aim of this paper is to design a NOMA-MIMO-VLC system, to achieve a low BER and a high data rate network. Moreover, the OFDM technique is used in the MIMO-VLC system that is proposed to maximize the spectral efficiency. Furthermore, a multi-user downlink NOMA-MIMO-VLC system is proposed with Equal Gain Combiner (EGC) at the receiver. The On–Off Keying (OOK) and *L*-Pulse Position Modulation (*L*-PPM) are adopted for performance analysis. The imperfect Successive Interference Cancellation (SIC) scenario is also considered to emphasize the practicability of the system, with both types: perfect and imperfect SIC. Our proposed DLMs are used to solve the complexity problem and over fitting, thereby improving our system performance. To evaluate the proposed model performance, the obtained data is divided into training and testing ones.

The regular steps to achieve our contribution of this research are as follows.

1. The NOMA-MIMO-VLC system in Dixit and Kumar (2022) is utilized to gain the advantages of transmitter and receiver diversity by applying the EGC techniques and the RC coding.
2. The SIC perfect and imperfect scenarios are considered.
3. Two modulation techniques are used; OOK and L-PPM.
4. The BER performance of the NOMA-MIMO-VLC system is used with system parameters as the diversity order, power allocation coefficient, α, and user count.
5. Two different DLMs are used to minimize the BER and maximize the spectral efficiency. Our proposed models are used to solve the complexity, over fitting problem, and to reduce the computational time, thereby improving our framework performance.

The organization of the paper is as follows. Section 2 describes the proposed system model. Section 3 lists the methodologies that are used. Section 4 displays and discusses the obtained results and analysis based on simulation and assessment parameters. Section 5 summarizes the findings and suggests some recommendations for a future research.

2 System model

Our proposed indoor VLC system is shown in Fig. 1. It consists of a room with dimensions (x, y, z) with two transmitters (LEDs) fixed on the ceiling at (x_1, y_1, h) and (x_2, y_2, h), where h is the height of the room. There is a K number of users and each user has M photodiodes (PDs) as receivers. Thus, each user is located at (x_{km}, y_{km}, h_r) m, where k and m are the user number and PDs number, $1 \le k \le K$, $m \in \{1, 2, \dots, M\}$, h_r is the height of the receiver. By this consideration, we achieve the MIMO technique, multiple input (two transmitters) and multiple output (K receivers). A Line of Sight (LoS) signal is considered and the Non-Line of Sight (NLoS) one is neglected which contains a negligible power (Dixit and Kumar 2020).

The transmitted signal from all LEDs are identical and are transmitted in the same time. Thus, $x_1 = x_2$, where x_1 is the transmitted signal from first LED and x_2 is the transmitted signal from second LED.

The received signal at the user is the summation of received optical power from both LEDs. As discussed, each user has number M photodiodes, so, at mth PD, where $m \in \{1, 2, \dots, M)$, the total received power can be expressed as

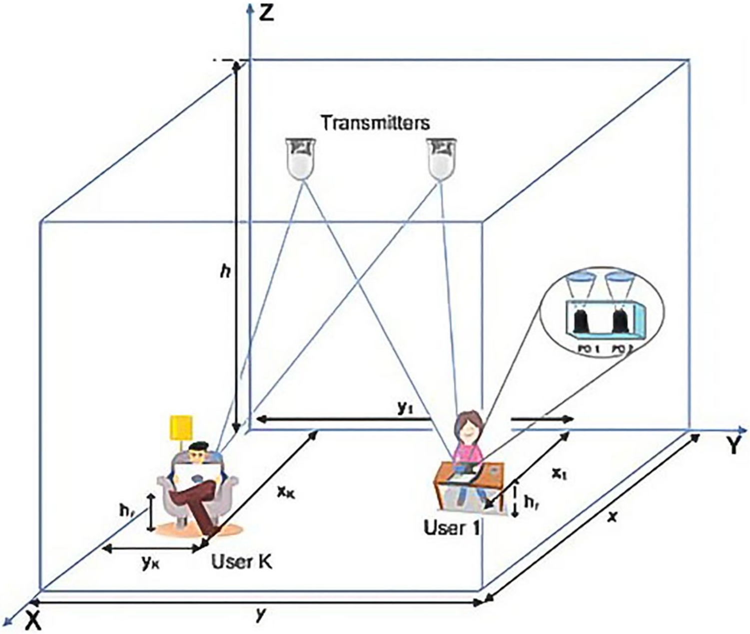

Fig. 1 NOMA-MIMO-VLC system model of user k

$$P_m^k = \sum_{n=1}^{2} \frac{P_t}{2} h_{mn}^k = P_{avg} \cdot \frac{P_t}{2} \tag{1}$$

where P_t and $P_{avg} = P_t/2$ are, respectively, the total and average transmitted power per LED and h_m^k is the channel gain at the mth PD, where

$$h_m^k = \sum_{n=1}^{2} h_{mn}^k \tag{2}$$

2.1 NOMA technique

Each user takes its number as user 1, user 2, … , user K. These numbers are ascendingly sorted related to the summation of channel gains received by M PDs in the user. Related to the concept of NOMA, the optical power assigned to the user has a descended ratio according to its position order. This means applying the fixed power allocation where the kth user is assigned power with

$$P_k = \alpha P_k + 1 \tag{3}$$

where α is the coefficient of power allocation, that is, $0 \leq \alpha \leq 1$.

So, the average power is

$$\sum_{k=1}^{K} P_k = P_{avg} \tag{4}$$

2.2 Perfect SIC decoding

SIC means successive interference cancellation between the users in our case. For example, if we have two users U1 and U2, then, the perfect SIC aims to cancel the interference at U1 related to U2 perfectly as shown in Dixit and Kumar (2022), where authors discussed mathematically the BER analysis.

When U2 is correctly decoded at U1 and hence, interference related to U2 will be cancelled out.

Perfectly, the BER of this case is given by

$$\mathrm{P}(\in_1^{(1)}= 1||| \in_2^{(1)}= 0) = \mathrm{P}(\in_1^{(1)}= 1)\mathrm{P}(\in_2^{(1)}= 0) = \mathrm{BER}_1^1\left(1 - \mathrm{BER}_1^2\right) \tag{5}$$

where $\mathrm{BER}^1{}_1$ and $\mathrm{BER}^2{}_1$ are the BER of self-decoding and decoding U2 at U1, respectively.

We solved this by using threshold detection method from Dixit and Kumar (2022), as

$$\mathrm{BER}_1^2 = 0.25 \times [2\mathrm{Q}(\chi_1\mathrm{P}_2) + \mathrm{Q}\left(\chi_1\left(\mathrm{P}_2 - 2\mathrm{P}_1\right)\right) + \mathrm{Q}\left(\chi_1\left(2\mathrm{P}_1 + \mathrm{P}_2\right)\right)], \tag{6}$$

$$\mathrm{BER}_1^1 = \mathrm{Q}(\chi_1\mathrm{P}_1) \tag{7}$$

$$\chi_2 = \mathrm{Rh}_2/\sqrt{\mathrm{M}\sigma_\mathrm{n}}. \tag{8}$$

$$\chi_1 = \mathrm{Rh}_1/\sqrt{\mathrm{M}\sigma_\mathrm{n}}. \tag{9}$$

where M is the total number of transmitters, h_1, h_2 are the channel gains LOS link for Users 1 and 2, respectively, R is the responsibility of the receiver photodiode, and σ_n is the variance at the mth PD of the user.

2.3 Imperfect SIC decoding

On the opposite side, the imperfect SIC means that there are some interferences as a result of incorrect decoding at U_1 related to U_2. Thus, interference is generated due to the incorrect decoding of U_2.

Also, authors in Dixit and Kumar (2022) discussed this case and analyzed the BER performance. The BER of this case is given by

$$\begin{aligned}\mathrm{P}(\in_1^{(2)}= 1||| \in_2^{(2)}= 1) = 0.25 \times [&\mathrm{Q}\left(\chi_1\left(\mathrm{P}_1 + 2\mathrm{P}_2\right)\right)\mathrm{Q}\left(\chi_1\mathrm{P}_2\right) + \mathrm{Q}(\chi_1(\mathrm{P}_1 - 2\mathrm{P}_2))\mathrm{Q}\left(\chi_1\mathrm{P}_2\right) \\ &+ \mathrm{Q}(\chi_1(\mathrm{P}_1 - 2\mathrm{P}_2))\mathrm{Q}(\chi_1(\mathrm{P}_2 - 2\mathrm{P}_1)) + \mathrm{Q}\left(\chi_1\left(\mathrm{P}_1 + 2\mathrm{P}_2\right)\right)\mathrm{Q}\left(\chi_1\left(2\mathrm{P}_1 + \mathrm{P}_2\right)\right)].\end{aligned} \tag{10}$$

3 Methodology

3.1 Dataset

Related to Dixit and Kumar (2022), we extracted the results from the figures as data sets to insert this data to DLM for training and adjusted the parameters to obtain the optimum performance according to a decreased BER with respect to signal to noise ratio (SNR). Table 1 demonstrates the extracted data sets with relation between BER and SNR.

3.2 Proposed DLMs

In our proposed framework, two different DLMs are performed to improve our framework performance through decreasing BER, complexity and increasing spectral efficiency. To solve various problems, pre-trained models are trained on a large benchmark dataset. In this paper, the DLMs are utilized to overcome the high complexity and over fitting, leading to improve the spectral efficiency. Different DLMs, ResNet50V2, and InceptionResNetV2 are introduced to enhance the performance.

3.2.1 Proposed DLMs, ResNet50V2, and InceptionResNetV2

The DLMs may have similar parameters. Many different layers' types are used in DLMs; max pooling and convolutional layers. While the input layer maintains the raw input data, the convolutional layer performs the dot product operation across all filters and data patches to compute the output volume. The activation function layer subjects the output of the first layer or the convolutional layer element by element. Additionally, the pool layer is in charge of reducing the volume and improving processing performance; both of which are input to the DLMs with the main objective of avoiding any kind of over fitting.

ResNet50V2 (Rizos and Kalogeraki 2020) is the ResNet50 upgrade version. This architecture is based on skip connections, which allow us to feed activation from one layer to the next. Inception-ResNet-v2 (Wang et al. 2021) is the inception mutual architecture with residual connections. Average pooling 2D is used to calculate the average for each patch of the feature map during the training process for ResNet50V2 and InceptionResNetV2 models. ResNet50V2 is a modified version of ResNet50 that performs better on our dataset than ResNet50 and ResNet101. ResNet50V2 performs better on our dataset than ResNet50 and ResNet101. The propagation formulation of the links between blocks was changed in ResNet50V2. Moreover, ResNet50V2 employs a more straightforward, single-scale processing unit with our datasets pass-through connections. While Multiple sized convolutional filters are mixed with residual connections in the InceptionResNetV2 block. The introduction of residual connections not only solves the degradation issue caused by deep structures, but it also shortens the training time. Furthermore, InceptionResNetV2 separates processing by scale, combines the outputs, and then repeats the process. Inception generates 1536 characteristics, whereas ResNet50V2 generates 2048. Based on previous explanation, it is observed that our proposed framework achieves the best performance with least complexity.

The parameters of the DLMs may be comparable. Each layer of a DLMs has the ability to transform one volume into another using a differentiable function. In our suggested system, the input layer stores the raw input matrix data, and the convolutional layer computes

Table 1 Data sets between BER and SNR (Dixit and Kumar 2022)

BER	SNR				
	U2 of 2 users based NOMA-MIMO-VLC	U3 of 3 users based NOMA-MIMO-VLC	U1 of 2 users based NOMA-MIMO-VLC	U1 of 3 users based NOMA-MIMO-VLC	U2 of 3 users based NOMA-MIMO-VLC
1×10^{-6}	130.5	133.5	133	0	137.5
2×10^{-6}	130.4444	133.4444	132.9778	15.55556	137.4444
3×10^{-6}	130.3889	133.3889	132.9556	31.11111	137.3889
3×10^{-6}	130.3333	133.3333	132.9333	46.66667	137.3333
3×10^{-6}	130.2778	133.2778	132.9111	62.22222	137.2778
3×10^{-6}	130.2222	133.2222	132.8889	77.77778	137.2222
3×10^{-6}	130.1667	133.1667	132.8667	93.33333	137.1667
3×10^{-6}	130.1111	133.1111	132.8444	108.8889	137.1111
3×10^{-6}	130.0556	133.0556	132.8222	124.4444	137.0556
3×10^{-5}	130	133	132.8	140	137
3×10^{-5}	129.8889	132.9444	132.7556	139.8889	136.9167
3×10^{-5}	129.7778	132.8889	132.7111	139.7778	136.8333
3×10^{-5}	129.6667	132.8333	132.6667	139.6667	136.75
3×10^{-5}	129.5556	132.7778	132.6222	139.5556	136.6667
3×10^{-5}	129.4444	132.7222	132.5778	139.4444	136.5833
3×10^{-5}	129.3333	132.6667	132.5333	139.3333	136.5
3×10^{-5}	129.2222	132.6111	132.4889	139.2222	136.4167
3×10^{-5}	129.1111	132.5556	132.4444	139.1111	136.3333
3×10^{-4}	129	132.5	132.4	139	136.25
3×10^{-4}	128.8889	132.3778	132.2889	138.9722	136.1667
3×10^{-4}	128.7778	132.2556	132.1778	138.9444	136.0833
3×10^{-4}	128.6667	132.1333	132.0667	138.9167	136
3×10^{-4}	128.5556	132.0111	131.9556	138.8889	135.9167
3×10^{-4}	128.4444	131.8889	131.8444	138.8611	135.8333

Table 1 (continued)

BER	SNR				
	U2 of 2 users based NOMA-MIMO-VLC	U3 of 3 users based NOMA-MIMO-VLC	U1 of 2 users based NOMA-MIMO-VLC	U1 of 3 users based NOMA-MIMO-VLC	U2 of 3 users based NOMA-MIMO-VLC
3×10^{-4}	128.3333	131.7667	131.7333	138.8333	135.75
3×10^{-4}	128.2222	131.6444	131.6222	138.8056	135.6667
3×10^{-4}	128.1111	131.5222	131.5111	138.7778	135.5833
3×10^{-3}	128	131.4	131.4	138.75	135.5
3×10^{-3}	127.8056	131.2222	131.2667	138.6111	135.3056
3×10^{-3}	127.6111	131.0444	131.1333	138.4722	135.1111
3×10^{-3}	127.4167	130.8667	131	138.3333	134.9167
3×10^{-3}	127.2222	130.6889	130.8667	138.1944	134.7222
3×10^{-3}	127.0278	130.5111	130.7333	138.0556	134.5278
3×10^{-3}	126.8333	130.3333	130.6	137.9167	134.3333
3×10^{-3}	126.6389	130.1556	130.4667	137.7778	134.1389
3×10^{-3}	126.4444	129.9778	130.3333	137.6389	133.9444
3×10^{-2}	126.25	129.8	130.2	137.5	133.75
3×10^{-2}	125.8889	129.4056	129.9	137.2222	133.3333
3×10^{-2}	125.5278	129.0111	129.6	136.9444	132.9167
3×10^{-2}	125.1667	128.6167	129.3	136.6667	132.5
3×10^{-2}	124.8056	128.2222	129	136.3889	132.0833
3×10^{-2}	124.4444	127.8278	128.7	136.1111	131.6667
3×10^{-2}	124.0833	127.4333	128.4	135.8333	131.25
3×10^{-2}	123.7222	127.0389	128.1	135.5556	130.8333
3×10^{-2}	123.3611	126.6444	127.8	135.2778	130.4167
3×10^{-1}	123	126.25	127.5	135	130

the output volume by performing the dot product operation over all filters and input patches. The output of the first layer or the convolutional layer is subjected to the activation function layer element by element. Furthermore, the pool layer is in responsibility of lowering volume and boosting processing performance, both of which are sent into the DLMs with the goal of avoiding overfitting. Moreover, our DLMs are trained by our collected data by dividing our datasets into 70% for training and 30% for testing and validation. Also, in the training stage, the DLMs are trained based on BER and SNR datasets. While, the in the testing stage, the input is SNR to predict the corresponding BER.

Furthermore, overfitting is a key concern when training our proposed framework using sample data. When the number of epochs utilized to train the model exceeds what is required, the training model learns patterns that are very unique to the sample data. As a result, the model is unable to perform well on a new dataset. The models perform well on the training set (sample data), but fail to perform well on the test set. In other words, by overfitting the training data, the models lose generalization capacity. The model should be trained for an ideal number of epochs to reduce overfitting and increase the capacity. A portion of the training data is dedicated to model validation, which is used to assess the model performance after each session of training. Loss and accuracy on both the training and validation sets are tracked to determine the epoch number at which the model begins overfitting. Therefore, our ideal epochs number are proposed in Table 2.

The activations are then flattened to create a vectorized feature map, and two fully connected layers are connected: one with 128 nodes and the other with 2-class classification (x, z). The second fully connected layer activations are then fed into a softmax layer, which calculates the probability for each coordinate (x, z). The parameters of the DLMs are explained in Table 2.

4 Results and discussion

Related to the derivation for BER in Dixit and Kumar (2022), the MIMO-NOMA-VLC system for two users and three users are numerically evaluated. Table 3 demonstrates the parameters used in the NOMA-MIMO-VLC system.

The users U1, U2, and U3 are placed indoor at the locations of (3, 3, 0.8) m, (3.5, 1.5, 0.8) m, and (1, 1, 0.8) m, respectively. The fixed power allocation coefficient, $\alpha = 0.2$. The users channel gain combination are in the range 5 to 10 related to what used in Dixit and Kumar (2022).

In this work we use two DL techniques: ResNet50V2 and InceptionResNetV2, for improving the performance of the NOMA-MIMO-VLC system. Generally, ResNet50V2 outperforms InceptionResNetV2 for different systems by ~ 6% improvement in different cases. The BER performance for two users OOK modulation: SISO, 2×2 and 3×2 MIMO-NOMA-VLC systems are simulated by both ResNet50V2 and InceptionResNetV2. Figure 2 shows the BER performance BER based on ResNet50V2. By comparing the results with those given in Dixit and Kumar (2022), we dedicate the improvement percentage for utilizing ResNet50V2 is nearly 15% for U2 and 8.6% for U1. Repeating the procedure by applying the InceptionResNetV2, that is displayed in Fig. 3, improvement of 3.4% for U1 and 5.8% for U2 and are noticed.

The BER performance versus α of the proposed systems based on ResNet50V2 InceptionResNetV2, respectively, is shown in Figs. 4 and 5. Related to the results in Dixit and Kumar (2022), applying ResNet50V2 in the system enhances the performance ~ 7.3%

Table 2 Parameters of DLMs

Setup	Learning rate	Optimizer	Activation function	Dropout	Batch size	Max pool size	Stride	Epoch
ResNet50V2	0.001	Adam with Alpha = 10^{-3}	Relu, Tanh	0.5	64	8×8	4×4	150
InceptionResNetV2	0.0001	SGD	Sigmoid	0.25	32	16×16	1×1	200

Table 3 Parameters used for NOMA-MIMO-VLC system (Dixit and Kumar 2022)

Description	Value	
Set-up parameters		
Room dimension	5 m×5 m×3 m	
Source parameters		
No. of LEDs (n)	2	
Source coordinates		
LED 1	2.5 m, 2.4 m, 3 m	
LED 2	2.5 m, 2.6 m, 3 m	
Semi-half angle of LED (φ1/2)	60°	
Receiver parameters	No. of PDs M = 2, 3. Locations	
	M = 2	M = 3
User-1 coordinates	PD1 (3, 2.95, 0.8) m	PD1 (3, 2.9, 0.8) m
	PD2 (3, 3.05, 0.8) m	PD2 (3, 3, 0.8) m
		PD3 (3, 3.1, 0.8) m
User-2 co-ordinates	M = 2	M = 3
	PD1 (3.5, 1.45, 0.8) m	PD1 (3.5, 1.4, 0.8) m
	PD2 (3.5, 1.55, 0.8) m	PD2 (3.5, 1.5, 0.8) m
		PD3 (3.5, 1.6, 0.8) m
User-3 co-ordinates	M = 2	M = 3
	PD1 (1, 0.95, 0.8) m	PD1 (1, 0.9, 0.8) m
	PD2 (1, 1.05, 0.8) m	PD2 (1, 1, 0.8) m
		PD3 (1, 1.1, 0.8) m
Active area of PD (A)	1 cm^2	
FOV (ψc)	60°	
Responsivity R	1 A/W	
Refractive index (ν)	1.5	
Gain of optical filter (T)	1	
Noise bandwidth (B)	50 MHz	
Transmission rate (Rb)	50 Mbps	

for U1 and ~ 9% for U2, while using InceptionResNetV2 achieves 3.5% improvement for U1 and 7.25% for U2.

The performance of three users OOK modulation SISO-NOMA-VLC, (2×2) and (3×2) SISO-NOMAVLC systems is shown in Figs. 6 and 7, based on ResNet50V2 and InceptionResNetV2, respectively. The InceptionResNetV2 outperforms the results in Dixit and Kumar (2022). In Fig. 6, an improvement of 26%, 205%, and 12.7% is achieved for U3, U2, and U1, respectively. While the corresponding improvement when using InceptionResNetV2, Fig. 7, is 20.9%, 20.3% and 9% for U3, U2, U1, respectively.

Figures 8 and 9 show the BER performance versus α of three users OOK modulation SISO and NOMA-MIMO-VLC; (2×2) and (3×2), based on ResNet50V2 and InceptionResNetV2 respectively. Utilizing ResNet50V2 outperforms the results in Dixit and Kumar (2022) with 9%, 6%, and 2.8% improvement for U3, U2 and U1, respectively. This improvement decreases when using InceptionResNetV2, where the improvement is 6%, 3%, and 1.5% for U3, U2 and U1, respectively.

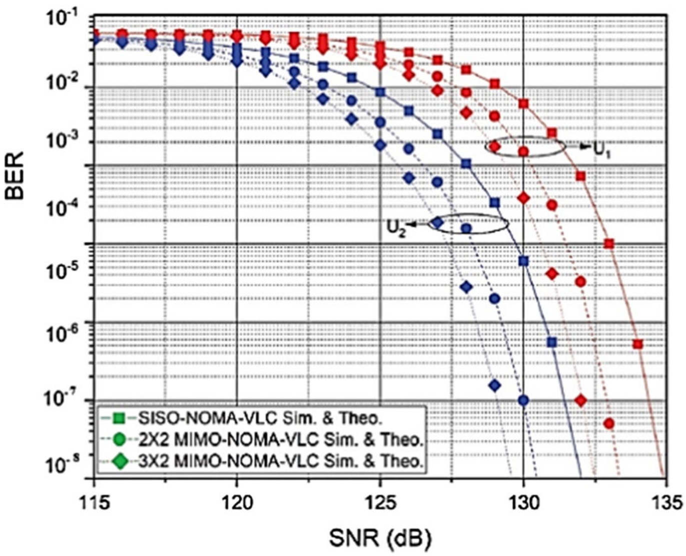

Fig. 2 BER performance for two users OOK modulation SISO and NOMA-MIMO-VLC system based on ResNet50V2

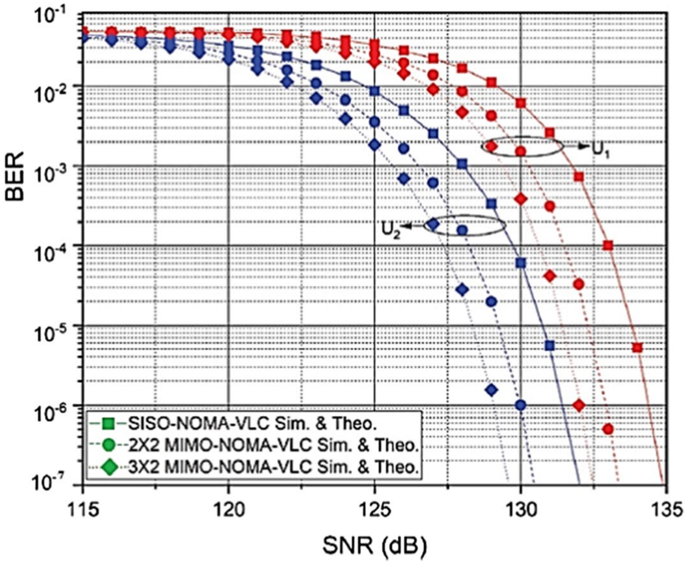

Fig. 3 BER performance for two users OOK modulation SISO and NOMA-MIMO-VLC system based on InceptionResNetV2

Figures 10 and 11 demonstrate a comparison for the BER performance of two users and three users OOK modulated NOMA-MIMO-VLC systems. Using ResNet50V2 and InceptionResNetV2 gain an improvement of 19% and 13%, respectively, if compared with the results (Dixit and Kumar 2022).

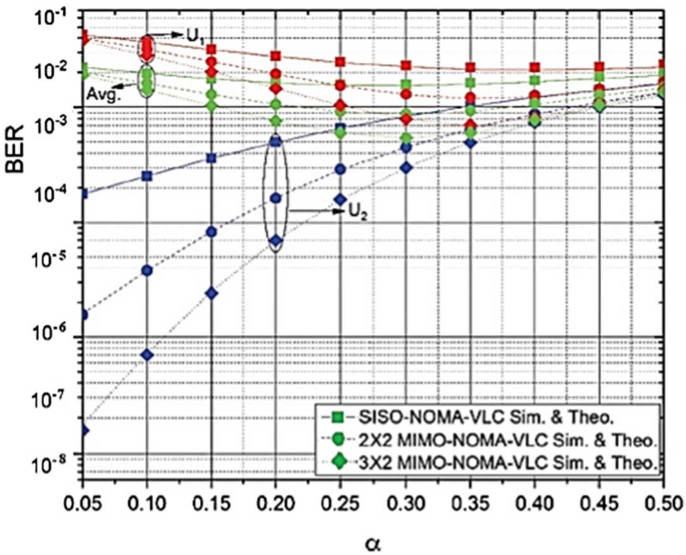

Fig. 4 BER versus α of two users OOK modulated SISO and MIMO-NOMA-VLC systems based on ResNet50V2

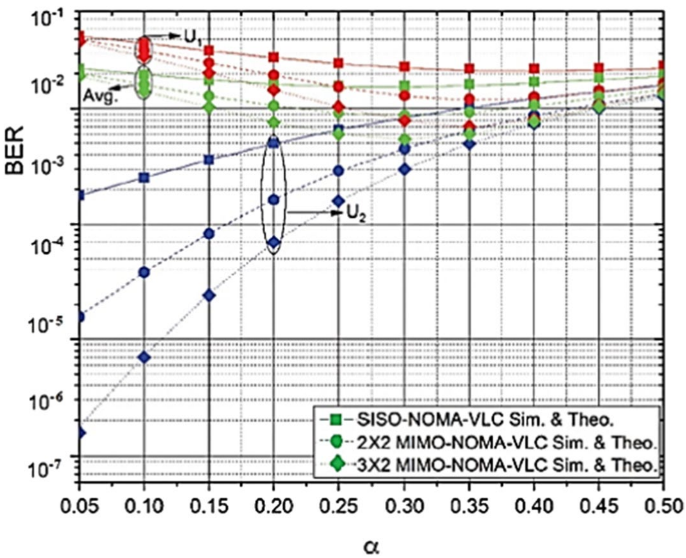

Fig. 5 BER versus α of two users OOK modulation SISO and MIMO-NOMA-VLC systems based on InceptionResNetV2

A BER comparison of two users OOK and L-PPM modulation NOMA-MIMO-VLC system is illustrated in Figs.12 and 13. The improvement percentage when using ResNet50V2, in Fig. 12, is 9.9% and is 5.3% when using InceptionResNetV2, Fig. 13.

The procedure is repeated in Figs. 14 and 15, showing a comparison for the BER comparison performance of two users and three users 4-PPM modulation NOMA-MIMO-VLC

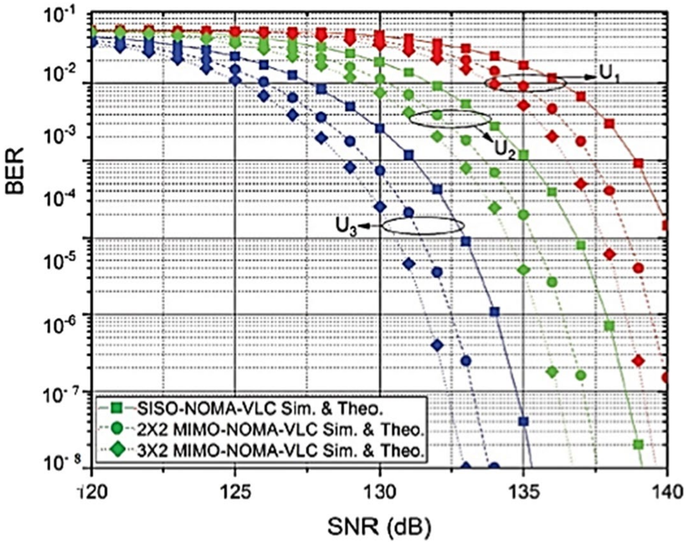

Fig. 6 BER performance of three users OOK modulation SISO and MIMO-NOMA-VLC systems based on ResNet50V2

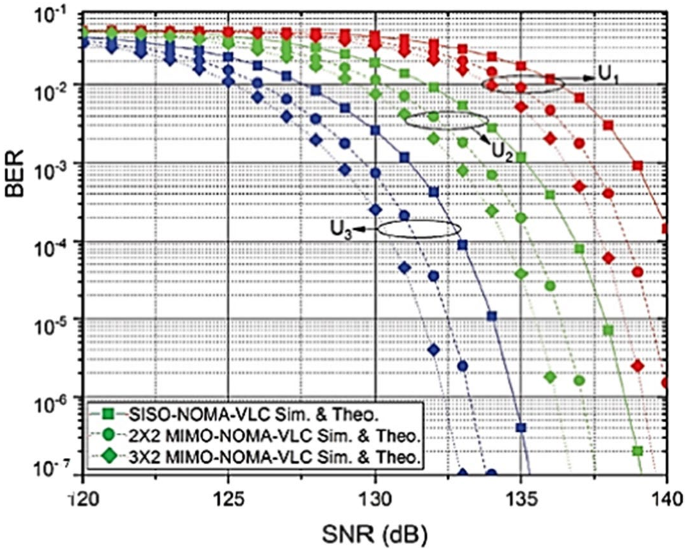

Fig. 7 BER performance of three users OOK modulation SISO and MIMO-NOMA-VLC systems based on InceptionResNetV2

systems. Based on ResNet50V2, Fig. 14, the improvement is 23% better than that found in Dixit and Kumar (2022) and is decreased to 15.8% when using InceptionResNetV2, Fig. 15.

Figures 16 and 17 display the BER performance versus α for two users and three users 4-PPM modulation NOMA-MIMO-VLC systems based on ResNet50V2 and

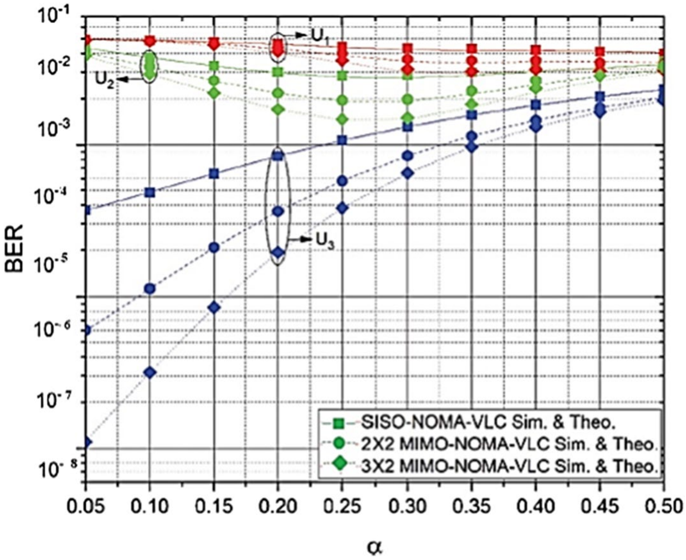

Fig. 8 BER performance versus α of three users OOK modulation SISO and MIMO-NOMA-VLC systems based on ResNet50V2

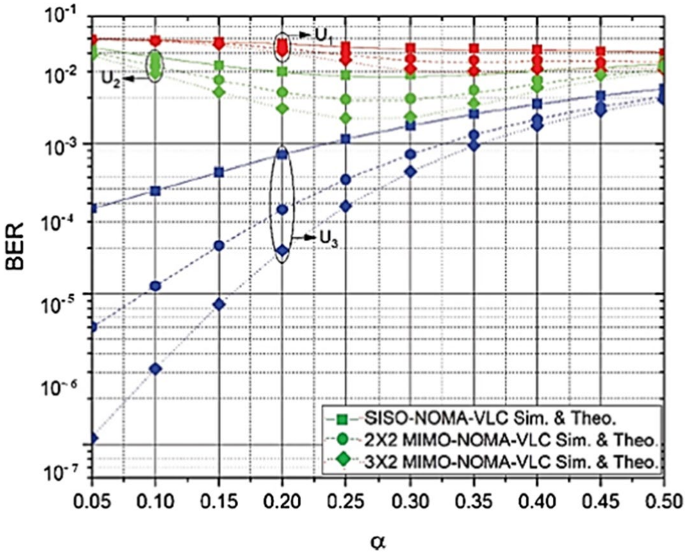

Fig. 9 BER performance versus α of three users OOK modulation SISO and MIMO-NOMA-VLC systems based on InceptionResNetV2

InceptionResNetV2. The improvement achieved is 16% and 10%, respectively, when utilizing ResNet50V2 and InceptionResNetV2.

The BER performance BER for two users OOK and L-PPM modulated NOMA-MIMO-VLC system is shown in Figs. 18 and 19, with perfect and imperfect SIC, based

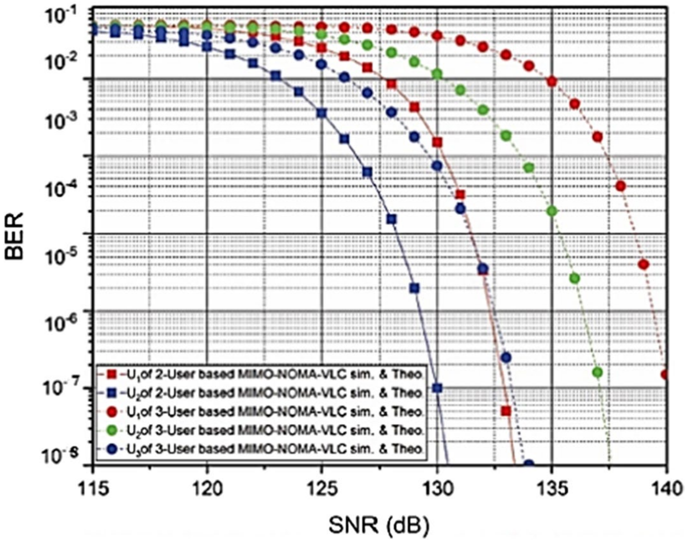

Fig. 10 BER performance: a comparison of two users and three users OOK modulated NOMA-MIMO-VLC system based on ResNet50V2

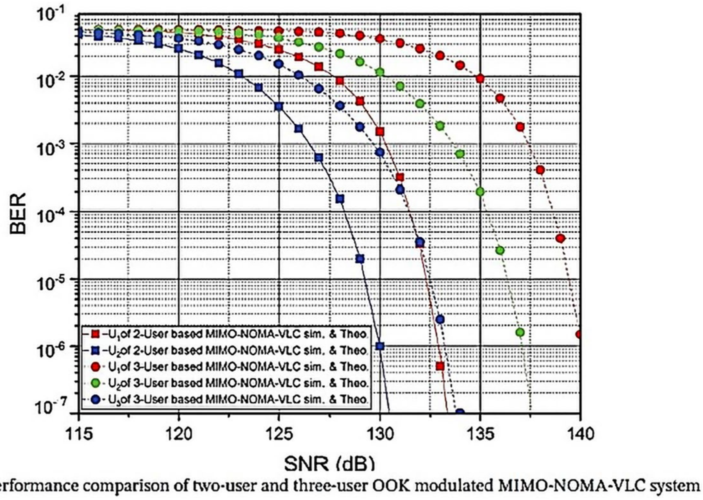

Fig. 11 BER performance: a comparison of two users and three users OOK modulated NOMA-MIMO-VLC system based on InceptionResNetV2

on ResNet50V2 and InceptionResNetV2, respectively. For the OOK modulation, an improvement of ~ 31% and ~ 24% is obtained when applying ResNet50V2 and InceptionResNetV2, respectively. Also, the 8-PPM outperforms other modulation techniques, showing an improvement of 36% and 20.4%, when using ResNet50V2 and InceptionResNetV2, respectively.

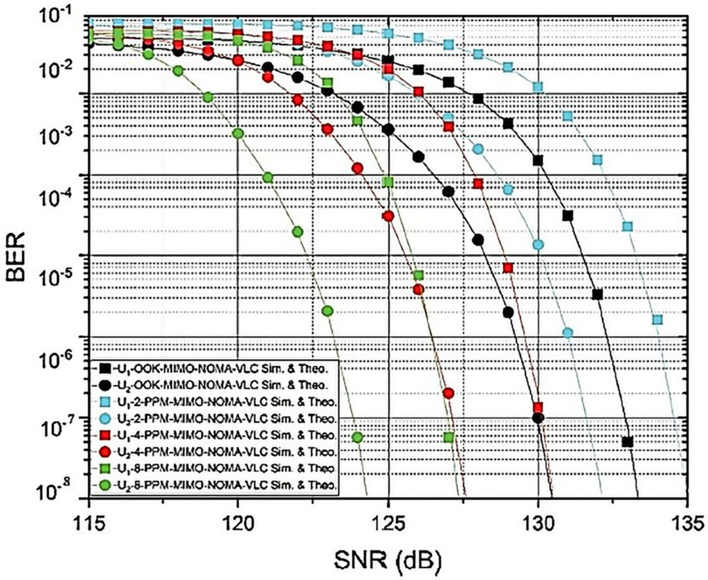

BER comparison of two-user OOK and *L*-PPM modulated MIMO-NOMA-VLC system

Fig. 12 BER comparison of two users OOK and L-PPM modulation NOMA-MIMO-VLC system based on ResNet50V2

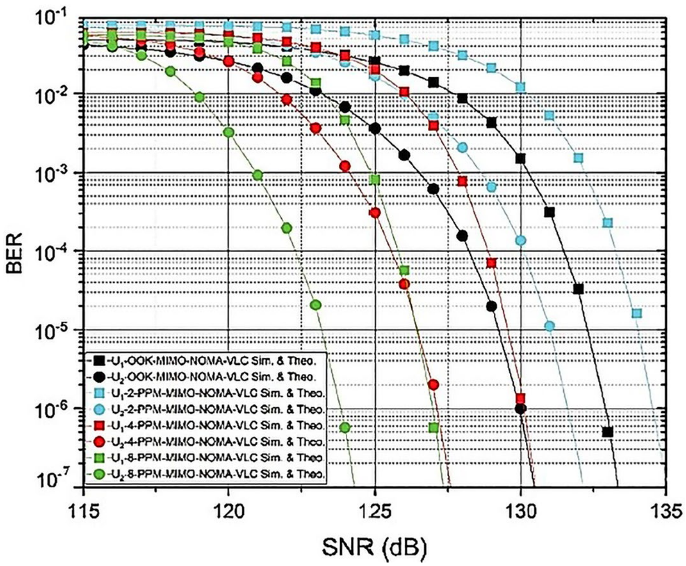

Fig. 13 BER comparison of two users OOK and L-PPM modulation NOMA-MIMO- VLC system Based on InceptionResNetV2

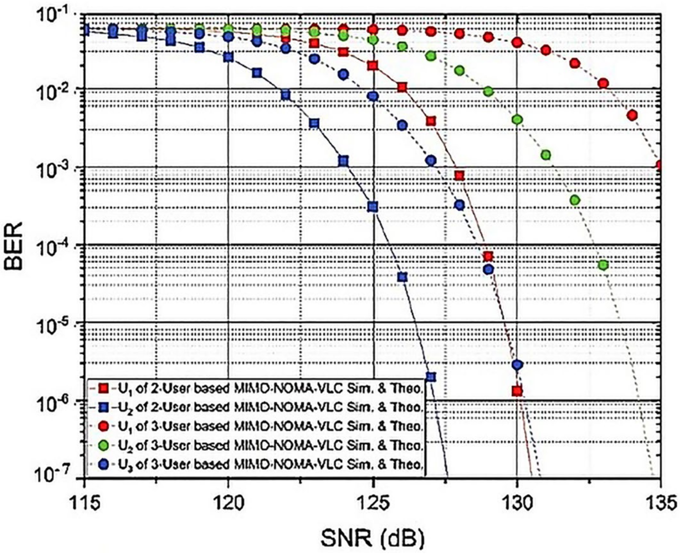

Fig. 15 BER performance: a comparison of two users and three users 4-PPM modulation NOMA-MIMO-VLC system VLC based on InceptionResNetV2

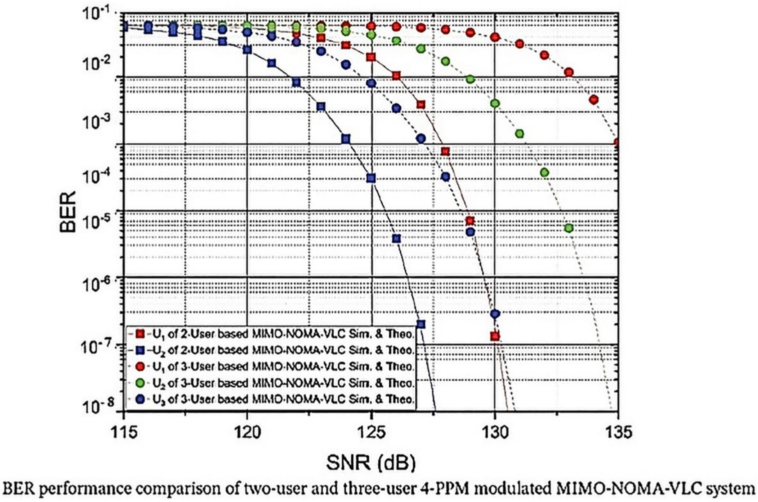

Fig. 14 BER performance: a comparison of two users and three users 4-PPM modulation NOMA-MIMO-VLC system VLC based on ResNet50V2

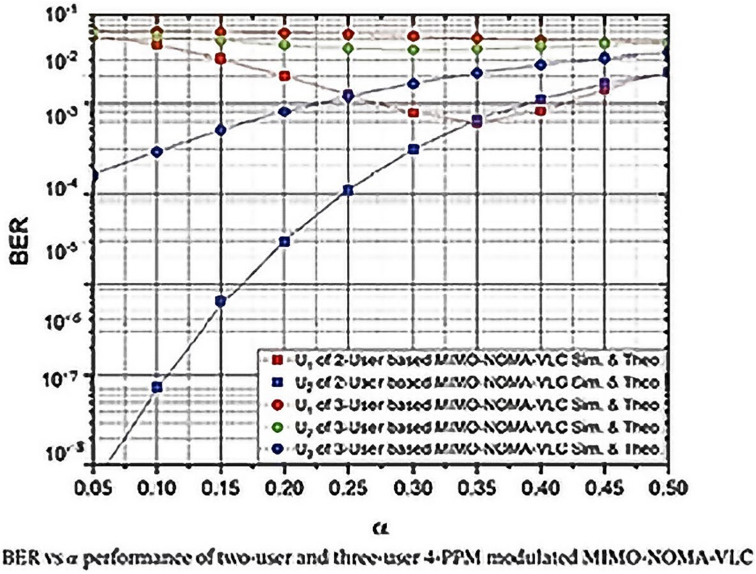

Fig. 16 BER versus α for two users and three 4-PPM modulation NOMA-MIMO-VLC based on ResNet50V2

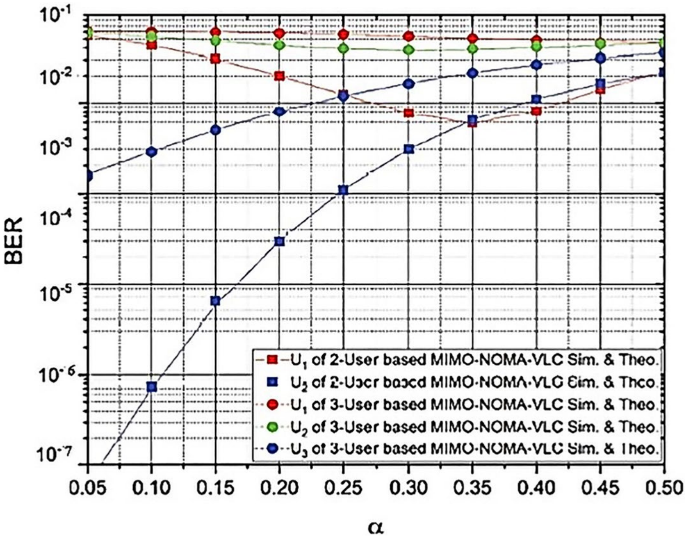

Fig. 17 BER versus α for two users and three 4-PPM modulation NOMA-MIMO-VLC based on Inception-ResNetV2

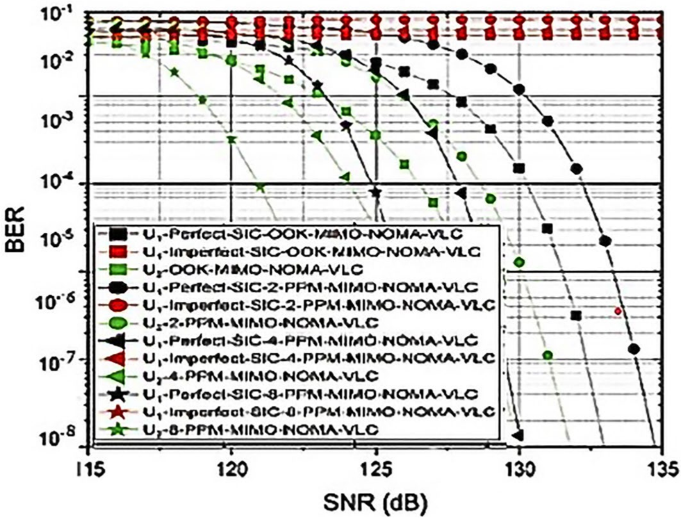

Fig. 18 BER performance for two users OOK and L-PPM modulation NOMA-MIMO-VLC system with perfect and imperfect SIC based on ResNet50V2

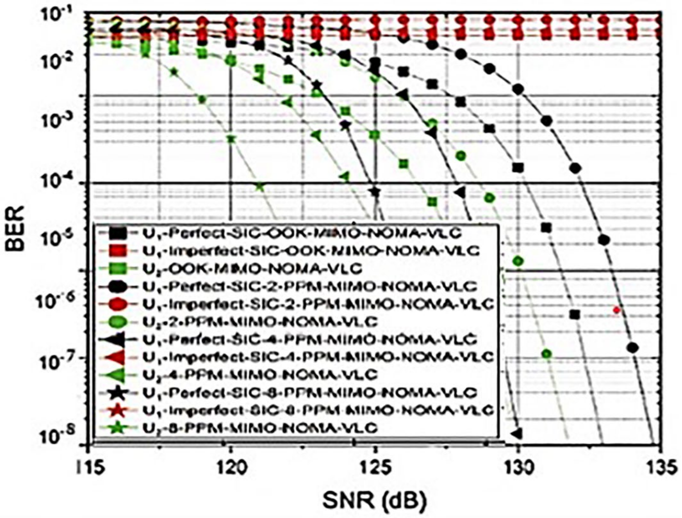

Fig. 19 BER performance for two users OOK and L-PPM modulation NOMA-MIMO-VLC system with perfect and imperfect SIC based on InceptionResNetV2

5 Conclusion

In this article, we utilize DL techniques; ResNet50V2 and InceptionResNetV2, for improving the performance of the NOMA-MIMO-VLC systems. The obtained results reveal that, in general, ResNet50V2 outperforms InceptionResNetV2 by nearly 6%. The BER performance for two users and three users OOK modulation SISO, 2×2 and 3×2 NOMA-MIMO-VLC systems are simulated by both ResNet50V2 and InceptionResNetV2. The obtained results are compared with that previously published ones, showing an enhancement in the performance for two users and three users systems.

The BER performance versus α is also investigated for two users and three users OOK modulation SISO and (2×2), (3×2) NOMA-MIMO-VLC systems based on ResNet50V2 and InceptionResNetV2. For two and three users, the performance is better enhanced when using ResNet50V2 than using InceptionResNetV2. The same notice is obtained also for the two users and three users 4-PPM modulation NOMA-MIMO-VLC system.

The improvement of using DL techniques is 16% and 10% when using ResNet50V2 and InceptionResNetV2, respectively. The BER performance is studied for two users OOK modulated NOMA-MIMO-VLC system with perfect and imperfect SIC, resulting in better improvement based on ResNet50V2 than InceptionResNetV2. The same conclusion, for both DL techniques, is achieved also when using 8-PPM which outperforms other modulation techniques.

Author contributions WMS, MHA, ESM have directly participated in the planning, execution, and analysis of this study. WMS drafted the manuscript. All authors have read and approved the final version of the manuscript.

Funding Open access funding provided by The Science, Technology & Innovation Funding Authority (STDF) in cooperation with The Egyptian Knowledge Bank (EKB). The authors did not receive any funds to support this research.

Data availability The data used and/or analyzed during the current study are available from the corresponding author on reasonable request.

Declarations

Conflict of interest The authors declare that they have no competing interests.

Ethical approval Not applicable.

References

Ai, J., Zhang, H., Zhang, Y., Lin, K., Zhang, Y., Wu, J., Wan, Y., Huang, Y., Song, J., Fu, Z., Wang, H.: Omicron variant showed lower neutralizing sensitivity than other SARS-CoV-2 variants to immune sera elicited by vaccines after boost. Emerg. Microbes Infect. **11**(1), 337–343 (2022)

Almohimmah, E.M., Alresheedi, M.T.: Error analysis of NOMA-based VLC systems with higher order modulation schemes. IEEE Access **8**, 2792–2803 (2020)

Al-Nahhal M., Basar E., Uysal M.: Adaptive unipolar MIMO-OFDM for visible light communications. In: Proceedings of the 2019 European Conference on Networks and Communications (EuCNC) pp. 73–77 (2019)

Al-Nahhal, M., Basar, E., Uysal, M.: Flexible generalized spatial modulation for visible light communications. IEEE Trans. Veh. Technol. **70**(1), 1041–1045 (2021)

An, Z., Zhang, T., Shen, M., De Carvalho, E., Ma, B., Yi, C., Song, T.: Series-constellation feature based blind modulation recognition for beyond 5g MIMO-OFDM systems with channel fading. IEEE Trans. Cognit. Commun. Netw. **8**(2), 793–811 (2022)

Bhatt, A., Shankar, R., Niedbala, G., Rupani, A.: Analysis of the fifth generation NOMA system using LSTM algorithm. Int. J. Comput. Digit. Syst. **11**(1), 215–223 (2022)

Chen, C., Zhong, W., Yang, H., Du, P.: On the performance of MIMO-NOMA-based visible light communication systems. IEEE Photon. Technol. Lett. **30**(4), 307–310 (2018)

Dixit, V., Kumar, A.: Performance analysis of non-line of sight visible light communication systems. Opt. Commun. **459**, 125008 (2020)

Dixit, V., Kumar, A.: An exact BER analysis of NOMA-VLC system with imperfect SIC and CSI. AEU Int. J. Electron. Commun. **138**, 153864 (2021a)

Dixit, V., Kumar, A.: Performance analysis of angular diversity receiver based MIMO–VLC system for imperfect CSI. J. Opt. **23**(8), 085701 (2021b)

Dixit, V., Kumar, A.: BER performance of MIMO based NOMA-VLC system with imperfect SIC. Trans. Emerg. Telecommun. Technol. **33**(4), e4422 (2022)

Kaur, R., Gholam Hosseini, H., Sinha, R., Lindén, M.: Melanoma classification using a novel deep convolutional neural network with dermoscopic images. Sensors **22**(3), 1134–1138 (2022)

Lin, B.: NOMA scheme for visible light communications using a single carrier transmission. In: Proceedings of the 1st South American Colloquium on Visible Light Communication (SACVLC), Santiago, pp. 1–4 (2017)

Liu, X., Chen, Z., Wang, Y., Zhou, F., Luo, Y., Hu, R.Q.: BER analysis of NOMA-enabled visible light communication systems with different modulations. IEEE Trans. Veh. Technol. **68**(11), 10807–10821 (2019)

Mitra, R., Bhatia, V.: Precoded Chebyshev-NLMS-based pre-distorter for nonlinear LED compensation in NOMA-VLC. IEEE Trans. Commun. **65**(11), 4845–4856 (2017)

Ngo, T.D., Bui, T.T., Pham, T.M., Thai, H.T., Nguyen, G.L., Nguyen, T.N.: Image deconvolution for optical small satellite with deep learning and real-time GPU acceleration. J. Real-Time Image Proc. **18**(5), 1697–1710 (2021)

O'Shea, T.J., Corgan J., Charles C.T.: Convolutional radio modulation recognition networks. In: Engineering Applications of Neural Networks: 17th International Conference, EANN 2016, 2013–2026, Aberdeen (2016)

Qi, W., Su, H.: A cybertwin based multimodal network for ECG patterns monitoring using deep learning. IEEE Trans. Ind. Inf. **18**(10), 6663–6670 (2022)

Rizos, P., Kalogeraki, V.: Deep learning for underwater object detection. In: 24th Pan-Hellenic Conference on Informatics, pp. 175–177 (2020)

Siddiqi, U.F., Narmanlioglu, O., Uysal, M., Sait, S.M.: Joint bit and power loading for adaptive MIMO OFDM VLC systems. Trans. Emerg. Telecommun. Technol. **31**, e3850 (2020)

Soltani, M., Pourahmadi, V., Mirzaei, A., Sheikhzadeh, H.: Deep learning-based channel estimation. IEEE Commun. Lett. **23**(4), 652–655 (2019)

Song, K., Yao, T., Ling, Q., Mei, T.: Boosting image sentiment analysis with visual attention. Neurocomputing **312**, 218–228 (2018)

Tian, W., Wang, S., Sun, S., Li, C., Lin, Y.: Intelligent prediction and early warning of abnormal conditions for fluid catalytic cracking process. Chem. Eng. Res. Des. **181**, 304–320 (2022)

Ullah, M.H., Gelli, G., Verde, F.: Visible light backscattering with applications to communication and localization in healthcare: a survey. Procedia Comput. Sci. **203**, 745–752 (2022)

Upadhya, A., Thakur, M.S., Sharma, N., Sihag, P.: Assessment of soft computing-based techniques for the prediction of Marshall stability of asphalt concrete reinforced with glass fiber. Int. J. Pavement Res. Technol. **15**(6), 1366–1385 (2022)

Wang, J., He, X., Faming, S., Lu, G., Cong, H., Jiang, Q.: A real-time bridge crack detection method based on an improved inception-resnet-v2 structure. IEEE Access **9**, 93209–93223 (2021)

Zaki, A.G., Hasanien, Y.A., El-Sayyad, G.S.: Novel fabrication of SiO_2/Ag nanocomposite by gamma irradiated *Fusarium oxysporum* to combat *Ralstonia solanacearum*. AMB Express **12**(1), 1–18 (2022)